Elastic Properties of Semi-Flexible Chains and Networks

*Peter Cifra, Tomáš Bleha**

Summary: Elastic properties of noncharged polymers of stiffness ranging from flexible to rigid chains are determined from Monte Carlo simulations. The discrete wormlike chain (WLC) model with self-interacting units is applied to chains of intermediate lengths. Elastic free energy and the force-extension profiles of chains of variable stiffness are computed in an isometric ensemble. Occurrence of a plateau on the force-extension curves at intermediate chain stiffness is noted. Qualitative differences are found between force profiles from simulations and from the standard (ideal) WLC model. The single-chain data on influence of bending stiffness were employed in the three-chain model of networks. Stress-strain relations for networks show a highly nonlinear behavior with the marked strain-stiffening effect.

Keywords: computer modeling; Monte Carlo simulations; networks; wormlike chains

Introduction

A central quantity characterizing elasticity of single macromolecules is the distribution function of the end-to-end distance $W(R)$. The distribution function $W(R)$, the related thermodynamic functions and force-extension curves are available from analytical calculations and computer simulations for a variety of chain models including the freely-jointed chain (FJC) and the wormlike chain (WLC) models.[1] The FJC model at low extensions reduces to the classical Gaussian model of random-coil elasticity, where the end-to-end distribution function $W(R)$ is given by the Gaussian function. A general solution of the function $W(R)$ in the WLC model became available only recently.[2,3]

In simulations of elastic properties of semiflexible macromolecules a discrete version of the WLC model is usually employed.[4,5] An inclusion of monomer-monomer self-interaction into a bead-spring chain model mimics the excluded-volume (EV) effect and variable solvent conditions. In contrast to charged macromolecules the self-avoidance effects may be of importance in noncharged semiflexible polymers, including aromatic amides, liquid crystalline polymers and polysaccharides.

In the paper we report the simulations of the behavior of noncharged polymers of stiffness ranging from flexible to almost rigid chains. The discrete WLC-like model involving self-interacting segments and the chain-end distance R as an independent variable (isometric boundary conditions) were employed. Influence of bending stiffness on elasticity of networks of semiflexible chains was investigated by the three-chain model of rubber-like elasticity.

Simulation Model

In a coarse-grained model, a semiflexible chain consists of beads connected by the effective bonds characterized by stiff springs. Each effective bond represents several chemical bonds along the chain backbone. An effective bond is described by finitely extensible nonlinear elastic potential (FENE)[6] involving the preferred bond distance l_o. Variations in chain stiffness are expressed by the bending

Polymer Institute, Slovak Academy of Sciences, 84236 Bratislava, Slovakia
Fax (+421)254775927
E-mail: bleha@savba.sk

potential[7] between two consecutive bonds which depends on the valence angle θ and the stiffness parameter b. Additionally, the discretized WLC model includes a Morse-type potential for interaction of pairs of effective units[6] that introduces the EV effect into the model. The principal parameters of the model are the chain stiffness b (related to the persistence length l_p) and the pair interaction energy ε. The parameters representing the good solvent condition were selected.

The chains of lengths from 20 to 400 units were generated. The Metropolis MC method with reptation updates of chains was used to obtain the ensemble averages. The stiffness parameter b was varied in the interval 0–75. The radial distribution function of end-to-end distances $P(R) = 4\pi R^2 W(R)$, the mean-square end-to-end distance $\langle R^2 \rangle$, and two WLC parameters, the contour length, $L_c = (N-1)\langle l \rangle$ and the persistence length l_p were evaluated from simulations. All values of the length quantities presented in Figures are normalized by the unit bond length $l_o = 0.7$.

Single-Chain Elastic Functions

Instead of the model-based stiffness parameter b the ratio of the contour and persistence lengths L_c/l_p will be employed as an indicator of the chain rigidity. This ratio of two experimentally accessible quantities is in a roughly reciprocal relation to the parameter b. The relation can be approximated by the allometric function $L_c/l_p = pb^q$, where $p = 85.79$ and $q = -0.941$ for $N = 100$. Conventionally, a chain is considered flexible when $L_c \gg l_p$ and rigid when $L_c \approx l_p$ holds. The semiflexible chains cover a wide range of parameters L_c/l_p between the above limits.

The distribution function $W(R)$ of a chain of contour length L_c is related to the free elastic energy $= c(T) - kT \ln W(R)$. The function $A(R)$ for chains of variable stiffness expressed by the ratio L_c/l_p is presented in Figure 1. The trends in the distribution functions and free energies observed for the self-interacting chain model are qualitatively similar to the findings reported[2–4] for the standard WLC model. A roughly Gaussian quadratic dependence of A on R is seen in Figure 1 in flexible chains, except at $R \to 0$ where, in contrast to ideal chains, the ring closure probability is zero due to the EV effect. With rising chain stiffness the minimum moves towards full chain stretching and a positive inclination of $A(R)$ curves in the central region changes to a negative one. A

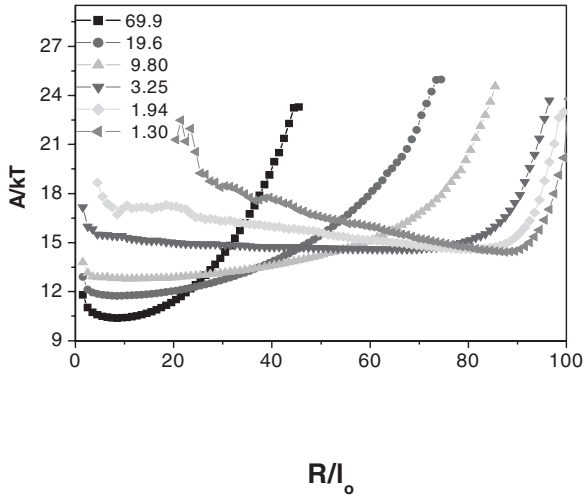

Figure 1.
Dependence of the elastic free energy on the chain extension R calculated for semiflexible chains of $N = 100$ at isometric conditions for chain stiffness L_c/l_p shown in the legend.

long, roughly flat section of the function $A(R)$ is observed in the crossover region between flexible and rigid chains. In this region a non-monotonic behavior of the functions $A(R)$ with double minimum hump was discovered in the standard WLC model[2,3] for a range of persistence lengths near to $L_c/l_p = 3.85$. Absence of such bimodality in Figure 1 could have a connection with the fact that the contour length is permitted to fluctuate in our discrete WLC-like model.

The mean force as a function of an independent variable R is determined by the differentiation $\langle f \rangle = dA/dR$. Forces and extensions are taken to be along the z axis. The curves $\langle f \rangle(R)$ markedly change along the transition from flexible to stiff chains and the highly nonlinear force-length functions are observed (Figure 2). A quasi-linear region of entropy elasticity is followed on curves by an upturn to higher forces. In stiff chains this upturn occurs at high extensions and becomes very steep. In flexible chains the compression forces ($\langle f \rangle < 0$) are present only at small R. However, in stiff chains the compressive force is predicted almost through all chain extensions. In harmony with the shape of elastic free energy $A(R)$ only one zero-force point (at finite extension) is present on each curve $\langle f \rangle(R)$ in Figure 2. In absence of the EV effect an additional zero-force point would be present at zero extension. Again, the zone of intermediate chain stiffness is worthy of note. In less stiff chains, with the ratio L_c/l_p above 4.06 ($b = 25$), a plateau is found in wide region of R featuring small positive mean forces. Below this crossover value of L_c/l_p such a plateau corresponds to small negative (compressive) forces. Around the end-to-end distance $\langle R^2 \rangle^{1/2}$ a force plateau changes to a force upturn.

Force-extension curves of semiflexible chains measured by the atomic force microscopy (AFM) methods are commonly interpreted by the WLC model using the approximate relation[8]

$$\frac{fl_p}{kT} = \frac{1}{4(1-x)^2} - \frac{1}{4} + x \qquad (1)$$

where $x = \langle R_z \rangle / L_c$ and $\langle R_z \rangle$ is the mean chain extension along the direction of the force. In derivation of this formula the force f was considered as an independent variable (the isotensional boundary conditions[9,10]). The formula accurately represents the small and large force regime but has a maximum error of 10% in the intermediate force regime. The force-extension profiles $\langle R_z \rangle$ *vs* f computed from the interpolation formula are compared in Figure 3 with curves $\langle f \rangle$ *vs* R from our isometric simulations. Significant differences are seen: first

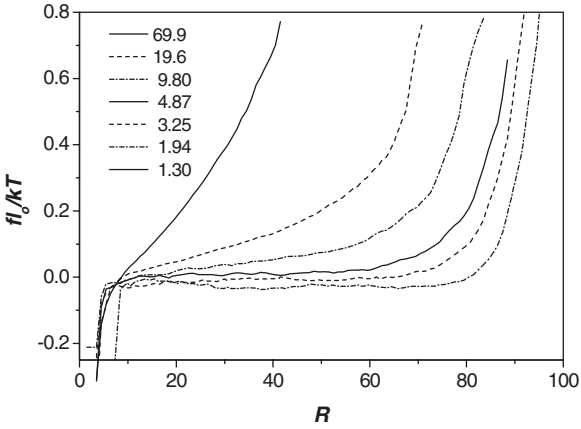

Figure 2.
Variation of the isometric mean force $\langle f \rangle$ with chain extension R calculated for the stiffness ratio L_c/l_p shown in the legend in the order of lines from left to right.

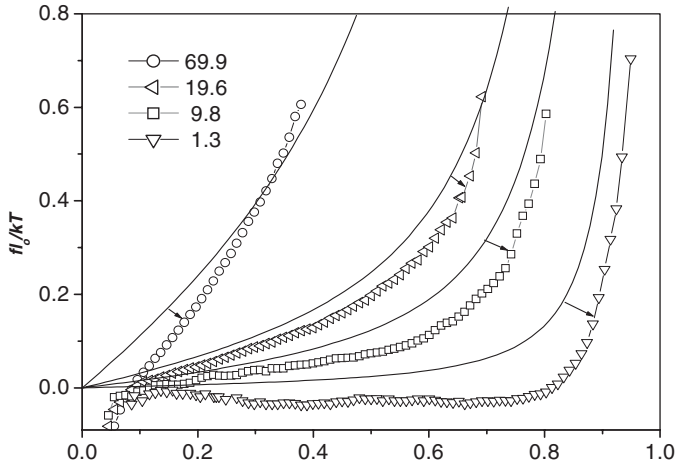

Figure 3.
Pairs of force-extension curves of semiflexible chains of $N = 100$ and the stiffness ratio L_c/l_p given in the legend computed from simulations at isometric conditions (symbols) and from the WLC interpolation formula (Equation 1).

of all, the WLC profiles are shifted to lower extension in comparison with the corresponding isomeric profiles from simulations. Then, only positive forces, all starting from origin, are present in the isotensional WLC profiles. Long plateau of nearly zero forces found in simulations in the crossover region at intermediate chain stiffness is missing in the WLC profiles. These differences become especially striking in stiff chains where simulations predict compressive forces up to very high chain extensions.

EV interactions and difference in boundary conditions assumed are the main factors contributing to disparity of curves in Figure 3 between our self-interacting WLC model and the standard (ideal) WLC model. In simulation curves in Figure 3 the EV effects are confined to low chain extensions R/L_c. A choice of a statistical ensemble has a more profound influence on elastic functions. Because of fluctuations in the measured lengths or forces on the single-molecule level, the $\langle f \rangle(R)$ relations are different from the $\langle R_z \rangle(f)$ relations even in a case of the structurally simplest polymer, polyethylene.[11] Only if fluctuations about the averages are ignored the designation of averages can be abandoned and the variables f and R can be transposed [1].

Semiflexible Networks

The single-chain elastic free energy and the functional dependence of the mean force $\langle f \rangle$ on R form a foundation of time-honored theories of network elasticity. The models based on the behavior of a set of ''average'' chains are conventionally used in computations of elastic properties of polymer networks.[12–14] The bending stiffness of chains introduces a new microscopic parameter that has a consequence for the traditional rubber-elasticity model of networks formed by crosslinked flexible polymers. It is frequently assumed that stiffening of network is ensuing primarily from longitudinal stiffening of polymer strands themselves.

The isometric single-chain functions presented in Figure 1 and 2 were utilized in the three-chain model of a network. This approach, exploited so far mostly for fully flexible chains[15–17] is supposed to be suitable also for semiflexible polymers. The model assumes that the free energies of chains are averaged in three orthogonal orientations. The effective chains with the

end-to-end distances R_i ($i = x,y,z$) parallel to the co-ordinate axes are deformed in the affine limit at constant volume, i.e. the crosslinks move linearly with the macroscopic dimensions of the sample L_i. The respective macroscopic deformations of a sample are defined as elongations $\lambda_i = L_i/L_{io}$ where subscript zero denotes the undeformed dimensions. In the case of uniaxial elongation ($\lambda_x = \lambda$ and $\lambda_y = \lambda_z = \lambda^{-1/2}$) the free energy A_{net} of a model network composed of ν chains per volume unit is given by the difference of the single-chain functions $A(R)$ in the deformed and undeformed state

$$A_{net} = \nu kT[A(R_o\lambda_x)/3 + (2/3)A(R_o\lambda_y) - A(R_o)] \quad (2)$$

where $R_o = \langle R^2 \rangle^{1/2}$ are the average chain dimensions of the network chains in the undeformed state.

The free energy of a model network A_{net} is plotted in Figure 4 as a function of elongation λ in wide range of chain stiffness. The free energy function of an ideal network of Gaussian chains, given by the relation $A_{G,net}/\nu kT = (1/2)(\lambda^2 + 2\lambda^{-1} - 3)$, is also shown in Figure 4. On rising stiffness one can see a stark reduction in degree of elongation λ, a sharp upturn in A_{net} and narrowing of a region around the free energy minimum. Interestingly, a similar pattern in variation of A_{net} was observed in simulations of model networks of helical polymers as a function of temperature.[18] It should be noted that in simulations with R as an independent variable the single-chain free energy minima in Figure 1 are not located at $R/R_o = 1$. This feature is also conserved at transformation of these data by means of Equation 2; the network free energy functions in Figure 4 are zero at $\lambda = 1$ but in most cases the minima of the functions are slightly displaced from this point.

The differentiation of Equation 2 with respect to elongation at constant volume and temperature gives the nominal stress σ as a function of isometric single-chain mean forces

$$\sigma = (\nu kTR_o/3) \times [f(R_o\lambda) - \lambda^{-3/2} f(R_o\lambda^{-1/2})] \quad (3)$$

The two terms in the brackets on the right-hand-side of Equation 3 account for the extension and lateral compression of the sample, respectively. The stress-strain relations computed for networks of chains of stiffness ranging from fully flexible to rather stiff polymers display numerous features of nonlinear elasticity (Figure 5). Extensibility of networks is drastically

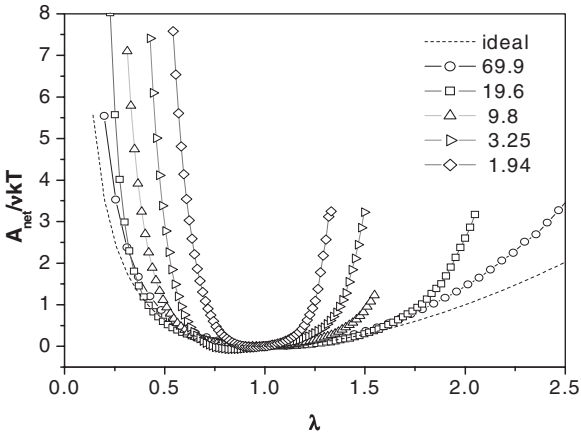

Figure 4.
The free energy of the three-chain model networks computed for chain stiffness L_c/l_p given in the legend. An analogous plot for an ideal network is shown by the dotted line.

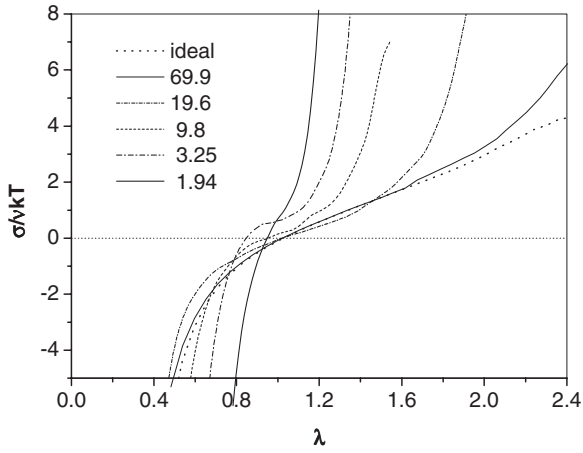

Figure 5.
Stress-strain relations of the three-chain model networks computed for stiffness L_c/l_p given in the legend (in the order from right to left). The ideal network relation is shown by the dotted line.

limited by increasing chain stiffness; an analogous compression effect is less pronounced in Figure 5. Similarly to Gaussian networks the deformation of networks of flexible chains is controlled mainly by entropy. On the other hand in stiffer chains, the deformation energy is stored primarily in bending of chain segments.

Interestingly, a force plateau featured in Figure 2 on single-chain curves $\langle f \rangle(R)$ in the crossover region of L_c/l_p is no more discernible on stress-strain isotherms of model networks. This hypothetical effect is effectively suppressed by the lateral compression term in Equation 3. Thus, the low-modulus elastic response of single chains in the region below and around $\lambda = 1$ is not transformed into an equivalent network behavior. The plots in Figure 5 corroborate the strain stiffening effect generic for networks composed of semiflexible polymers. The strain at which stiffening becomes significant strongly depends on the persistence length. It is encouraging that stress-strain relations in Figure 5 qualitatively agree with the results of MC simulations for a more complex and realistic model of end-linked networks of semiflexible chains.[19]

It should be mentioned, however, that the simple model used is suitable just to networks made from not too rigid chains, with little or no entanglements. Numerous inherent limitations of the three-chain model preclude its applicability to very stiff networks and to entangled networks. For example, nematic mean-field type of interaction is needed in networks made from semi-rigid chains where it leads to the appearance of an isotropic - nematic transitions at high strains.[20] Furthermore, it is supposed that in flexible polymers segments between crosslinks behave independently. However, strands in semiflexible networks most likely act in series, since segments of stiff chains remain correlated over much longer distances that is the mesh size of a crosslinked network. Thus the properties of such a network depend both on mesh size and the contour length of chains.[21]

Conclusions

A segmental model involving self-avoiding and interacting units, corresponding to a discretized WLC model, was employed in Monte Carlo simulations of chains of stiffness ranging from the fully flexible to relative stiff polymers. Stiffness-induced modifications of the elastic free energy and force-extension curves computed in an isometric ensemble were presented. At intermediate chain stiffness a long plateau

on the force-extension curves was observed. Qualitative differences are found between the force profiles from simulations and from the standard (ideal) WLC model. The differences can be ascribed to an inherent dissimilarity of the isometric and isotensional ensembles and, at small extensions, to the excluded volume effects.

Influence of bending stiffness, a new microscopic parameter in traditional rubber-like network elasticity, was explored by the three-chain model. It was found that extensibility of networks is drastically reduced by increasing chain stiffness; an analogous compression effect is less pronounced. The stress-strain isotherms show a highly nonlinear behavior with the marked strain-stiffening effect.

Acknowledgements: This work was supported by Science and Technology Assistance Agency under the contract No. APVT-51-044902 and in part by VEGA, Grant 2/6014/26.

[1] P. J. Flory, "*Statistical Mechanics of Chain Molecules*", Wiley - Interscience, New York 1969.
[2] J. Samuel, S. Sinha, *Phys. Rev. E* **2002**, *66*, 050801.
[3] A. Dhar, D. Chaudhuri, *Phys. Rev. Lett.* **2002**, *89*, 065502.
[4] R. G. Winkler, *J. Chem. Phys.* **2003**, *118*, 2919.
[5] J. M. Kneller, C. Elvingston, G. A. Arteca, *Chem. Phys. Lett.* **2005**, *407*, 384.
[6] A. Milchev, K. Binder, *Macromolecules* **1996**, *29*, 343.
[7] P. Cifra, *Macromolecules* **2005**, *38*, 3984.
[8] J. F. Marko, E. D. Siggia, *Macromolecules* **1995**, *28*, 8759.
[9] H. J. Kreuzer, S. H. Payne, L. Livadaru, *Biophys. J.* **2001**, *80*, 2505.
[10] D. Keller, D. Swigon, C. Bustamante, *Biophys. J.* **2003**, *84*, 733.
[11] M. Zemanová, T. Bleha, *Macromol. Theory Simul.* **2005**, *14*, 596.
[12] L. R. G. Treloar, "*The Physics of Rubber Elasticity*", Claredon Press, Oxford UK 1975.
[13] J. E. Mark, J. G. Curro, *J. Chem. Phys.* **1983**, *79*, 5705.
[14] J. I. Cail, R. F. T. Stepto, *Polymer* **2003**, *44*, 60.
[15] J. E. Mark, *J. Phys. Chem. B* **2003**, *107*, 903.
[16] P. Cifra, T. Bleha, *Macromolecules* **1998**, *31*, 1358.
[17] P. Cifra, T. Bleha, *J. Polym. Sci. Polym. Phys.* **1999**, *37*, 2013.
[18] G. A. Carri, R. Batman, V. Varshney, T. Dirama, *Polymer* **2005**, *46*, 3809.
[19] D. M. Bhawe, C. Cohen, F. A. Escobedo, *Macromolecules* **2004**, *37*, 3924.
[20] I. Bahar, B. Erman, A. Kloczkowski, J. E. Mark, *Macromolecules* **1990**, *23*, 5341.
[21] D. A. Head, A. J. Levine, F. C. MacKintosh, *Phys. Rev. E* **2003**, *68*, 061907.

